First-principles modeling of intrinsic and extrinsic defects in γ-Al$_2$O$_3$

K. Sankaran,[1,2,a)] G. Pourtois,[1,3] R. Degraeve,[1] M. B. Zahid,[1] G.-M. Rignanese,[2] and J. Van Houdt[1]

[1] IMEC, Kapeldreef 75, B-3001 Leuven, Belgium
[2] European Theoretical Spectroscopy Facility (ETSF) and Institute of Condensed Matter and Nanosciences (IMCN), Université catholique de Louvain, 1 Place Croix du Sud, 1348 Louvain-la-Neuve, Belgium
[3] Department of Chemistry, PLASMANT Research Group, University of Antwerp, Universiteitsplein 1, B-2610 Wilrijk-Antwerp, Belgium

The electronic properties of a set of intrinsic and extrinsic point defects in γ-Al$_2$O$_3$ are investigated using quasiparticle calculations within the G$_0$W$_0$ approximation. We find that the electronic signature of atomic vacancies lie deep in the band gap, close to the top of the valence band edge. The introduction of C, Si, and N impurities induces defective levels that are located close to the conduction band edge and near the middle of the band gap of the oxide. The comparison with electrical measurements reveals that the energy levels of some of these defects match with the electronic fingerprint of the defects reported in γ-Al$_2$O$_3$ based nonvolatile memories. © 2010 American Institute of Physics. [doi:10.1063/1.3507385]

The aggressive reduction of the thickness of the silicon native oxide as gate dielectrics for logic and memory devices has been reviving fundamental concerns about the possible increase of the leakage current. As a result, alternative materials with higher dielectric constant (high-κ) than SiO$_2$ have been thoroughly investigated.[1] Due to specific working operations, the requirements are very stringent on the dielectric to be used in non-volatile memory flash based devices: large band gaps and band-offsets combined with low trap densities are needed.[2] Typically, the dielectric constant of the materials targeted should range from 9 to 20, while showing a large band gap value (ideally between 6.5 and 9 eV). Naturally, these high-κ oxides ought to offer the same properties in terms of stability, low defect concentration and data retention as SiO$_2$. So far, such requirements have not been met.

Recently, Al$_2$O$_3$ has received considerable attention as a possible replacement for SiO$_2$ in the future generation of flash memories.[3] While α-Al$_2$O$_3$ is the most stable crystal phase, independently of the pressure and temperature conditions, several metastable phases known as κ and γ-Al$_2$O$_3$ also exist. Among these three different polymorphs, γ-Al$_2$O$_3$ displays the most interesting properties. It crystallizes at relatively low temperatures [from 350 to 1000 °C (Ref. 4)] and it is able to maintain its crystalline phase up to temperatures as high as 1200 °C,[5] which makes it compatible with the standard processing techniques used in the microelectronic industry. From an electronic point of view, the band gap of γ-Al$_2$O$_3$ is about 7.0 eV,[6] which is lower than for all the other existing polymorphs but perfectly suited for nonvolatile memory applications.

As a consequence, γ-Al$_2$O$_3$ has been introduced as a dielectric in TaN(TiN)/γ-Al$_2$O$_3$/Si$_3$N$_4$/SiO$_2$/Si (TANOS) flash memories.[7] Unfortunately, the material displays substantially more electron traps than SiO$_2$, which act detrimentally for the reliability of the memory.[8] Recent trap spectroscopy by charge injection and sensing (TSCIS) and photoinjection-photodepopulations measurements[9,10] have

revealed the presence of two sets of defects located at 1.6–2.0 and 2.6–3.6 eV below the conduction band edge of γ-Al$_2$O$_3$. These traps are believed to be at the origin of the reliability issues reported by Kerber et al.[8] A proper integration of γ-Al$_2$O$_3$ requires overcoming these concerns and hence necessitates a thorough understanding of the nature of the detected electronic defects. In this context, it is important to be able to obtain a good prediction of the defect properties, particularly the defect energy levels. Therefore, to gain some insight into the nature of the defects observed experimentally, we modeled the electronic signatures of a set of possible intrinsic (O and Al vacancies) and extrinsic defects within the many-body peturbation theory (MBPT) formalism.

Computing the position of the defective levels in the electronic gap of a solid is not a trivial task for typical first-principles modeling techniques. The most commonly used theoretical approach is the density functional theory (DFT). However, while it is generally observed that DFT predicts structural properties within a few percent of the experimental values, its predictive power is notoriously limited as far as electronic properties are concerned. This is due to intrinsic deficiencies of the semilocal approximations to DFT—such as the local density approximation or the generalized-gradient approximation (GGA)—that lead to a pathological underestimation of the band gap.[11] In this respect, orbital-dependent approaches[12] and MBPT[13] have brought a significant improvement. While the former may be less computationally demanding, their reliability cannot be assessed a priori[12] in contrast with MBPT.

In this paper, the structural properties (lattice shape and atomic positions) are fully relaxed at the DFT level, while the electronic properties are obtained from MBPT, both using the ABINIT package[14] relying on the projected augmented wave method.[15] In the DFT calculations, the exchange-correlation energy is described within the GGA using the Perdew–Burke–Ernzenof (PBE) functional.[16] The quasiparticle corrections are obtained using the DFT eigenenergies and wave functions as an input to generate the self-energy in the G$_0$W$_0$ approximation. For all the systems, both the kinetic

a)Electronic mail: sankaran@imec.be.

energy (24 Ha) and the Monkhorst–Pack grid (a $4 \times 4 \times 2$ k-point mesh) are chosen to ensure a good convergence of the calculated properties. In the G_0W_0 calculations, the dielectric matrix $\varepsilon^{-1}(\mathbf{G}, \mathbf{G}')$ is computed in the random-phase approximation, including 150 empty states in the summations, only for $\mathbf{G}$ vectors with a kinetic energy smaller than 6 Ha. The dynamic dependence of ε^{-1} was approximated using a plasmon-pole model[17] fitted to the actual calculated values at two imaginary frequencies. The self-energy was obtained by summing over 150 unoccupied bands. These parameters ensure quasiparticle corrections converged to less than 0.05 eV. There are many controversial literature reports concerning the structures of γ-Al$_2$O$_3$ due to confusion in the distribution of O vacancies.[18] In this work, we used the model proposed by Menéndez *et al.*, in which the crystal is derived from a defective spinel structure.[19] The unit cell consists of 40 atoms in which Al atoms occupy both octahedral and tetrahedral sites in a 5:3 ratio, while the O atoms are three- and fourfold coordinated. The accuracy of the description of the electronic properties of bulk γ-Al$_2$O$_3$ was validated by comparing the computed band gap energy computed at the PBE (4.4 eV) and G_0W_0 (7.2 eV) levels to the experimental one (7.0 eV).[20] γ-Al$_2$O$_3$ has a direct band gap at Γ point, which is defined by the highest occupied valence band (O $2p$ states) and by the lowest unoccupied conduction band (Al $3s$ and $3p$ states). As expected, the G_0W_0 corrections improve significantly the description of the electronic gap and set it at about 0.2 eV of the experimental value (7.0 eV). Note that, for all the systems, the position of the defect level in the band gap was checked with respect to the number of unit cells used in order to quantify the impact of the spurious interaction of the defects in neighboring cells. It turns out that an accuracy of 0.1 eV on the level position is reached already with a single unit cell.

By symmetry, the γ-Al$_2$O$_3$ crystal only displays four nonequivalent atomic sites hereafter denoted O$_3$, O$_4$, Al$_4$, and Al$_6$ (corresponding to oxygen or aluminum atoms three-fold, fourfold, or sixfold coordinated). A series of models with either an O vacancy (V_O) or an Al(V_{Al}) vacancy is first generated by removing a single oxygen or aluminum atom on one of these sites and subsequently relaxing the structure. It is found that the presence of the vacancies has little impact on the crystal structure. In order to be as consistent as possible with the nature of the film characterized in Refs. 9 and 10 another series of models accounts for the possible substitution of the Al or O species during the growth by either a residue of the C-based precursor, N due to the post-deposition thermal treatment in a nonreacting ambient or Si that has diffused from the substrate (induced by the high temperature post-deposition anneal treatment). Note that we focused on the signatures of atomic vacancies and on the possible chemical substitutions rather than on the interstitials and grain boundaries related issues to maintain the G_0W_0 simulations computationally tractable.

Since O vacancies have been reported to be predominant in high-κ dielectric materials,[21] we first studied their electronic signatures in γ-Al$_2$O$_3$. Note given the similarity of the results obtained for the V_{O3} and V_{O4}, the discussion hereafter is restricted to the V_{O4} case. The presence of neutral O vacancy (V_O) induces two electronic states that are doubly occupied and lie close to the valence band (VB), at about 6.9 and 6.5 eV below the conduction band (CB) edge of γ-Al$_2$O$_3$
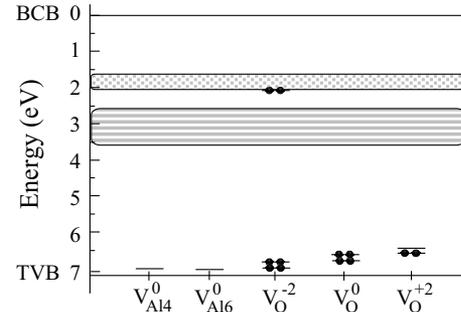

FIG. 1. Distribution of the electronic levels associated to an O and Al vacancy in γ-Al$_2$O$_3$ between the top of the valence band (TVB) and the bottom of the conduction band (BCB). The dotted and striped regions represent the positions of the traps reported experimentally (Refs. 9 and 10).

(Fig. 1). Taking into account the CB offset between the Si substrate and γ-Al$_2$O$_3$ [2.8 eV (Ref. 22)] it is found that the V_O^0 levels lie below the VB edge of Si, suggesting that the vacancy is able to trap a charge. The investigations were hence extended to the case of charged O vacancies, as suggested for low density alumina models.[21,23] Upon electron trapping, a new doubly occupied state (V_O^{2-}) appears above the middle of the gap value, while in presence of a positive charge (V_O^{2+}), the electronic levels are shifted upwards in the band gap compared to V_O^0. Interestingly, the occupied level associated to V_O is found to lie closer to the top of the VB (by about 3 eV) than for the Al$_2$O$_3$ phase built on the β-Ga$_2$O$_3$ symmetry (hereafter denoted as built-β-Al$_2$O$_3$ for simplicity) by Liu *et al.*[21] We attribute this difference to the change in coordination adopted by the Al centers when going from the γ (32.5% of Al fourfold coordinated) to the "built-β" phase (50% of Al fourfold coordination). Interestingly, the trapping of two electrons on an O vacancy site (V_O^{2-}) induces an electronic level that corresponds to one of the signatures (1.6–2.0 eV) detected by TSCIS. However, it cannot explain the second peak detected at lower energies (2.6–3.6 eV) in the band gap.[10] The introduction of Al vacancy in both Al$_4$ and Al$_6$ sites (V_{Al4} and V_{Al6}) generates acceptorlike levels that lie deep in the band gap, close to the VB edge of γ-Al$_2$O$_3$ (Fig. 1).

None of the defects considered so far, is sufficient to explain the distribution observed experimentally for the two electronic levels.[9,10] In contrast, the generation of extrinsic defects (C, Si, and N) provides an interesting insight into the signatures measured electrically. It turns out that the presence of these impurities induces a distribution of electronic levels in the band gap of γ-Al$_2$O$_3$ (Fig. 2) whose positions are driven by both the coordination and the nature of the chemical impurities. Taking the CB offset (2.6 eV) between Al$_2$O$_3$ and Si into account, it is found that numerous fully- and partially-empty levels are accessible for an electron trapping process. However, a one-to-one comparison of the position of the electronic levels with the experimental distribution suggests that most of these defects do not correspond to the detected signature. For instance, the N_{O3}, N_{O4}, N_{Al4}, and N_{Al6} substitutions generate a set of levels that lie out of the boundaries of the detected signals, implying that nitrogen is not at the origin of the reduction in retention time of the TANOS system. A similar statement can be made for the C substitution in γ-Al$_2$O$_3$, where the computed levels are not consistent with the position of the experimental bands.
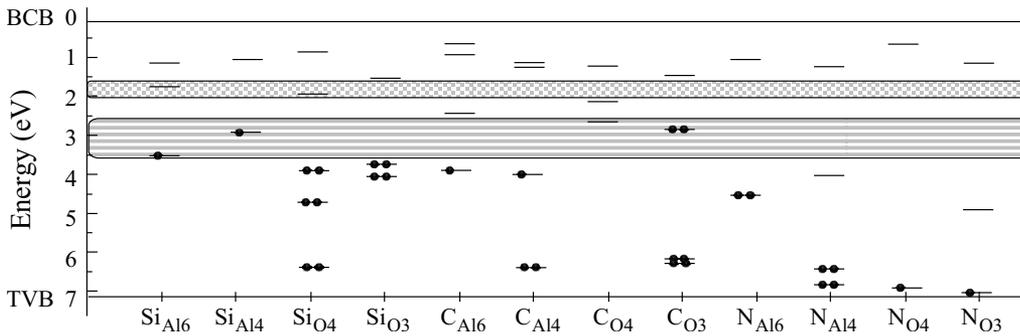
FIG. 2. Distribution of the electronic levels associated to different extrinsic defects in γ-Al_2O_3 between the top of the VB (TVB) and the bottom of the CB (BCB). The dotted and striped regions represent the positions of the traps reported experimentally (Refs. 9 and 10).

Interestingly, the substitution Si_{Al6} in γ-Al_2O_3 generates three electronic levels: one partially filled (singly occupied) at 3.5 eV of the CB of the oxide, which is in good agreement with the position reported experimentally (from 2.6 to 3.6 eV from CB edge of the oxide) and two other empty ones (ranging from 1.1 to 1.7 eV below the CB of γ-Al_2O_3), whose locations correspond to the band observed experimentally from 1.6 to 2.0 eV. Note that when transferring the substitution site from Al_6 to Al_4, a single filled electronic level appears at about the same energy as the experimental band observed at 2.9 eV below the CB but the presence of another electronic level (about 1.1 eV below the CB) does not fit the experimental band ranging from 1.1 to 1.7 eV. In this specific case, the Al_6 centers can accommodate the presence of a defect much more easily than the Al_4 ones due the higher degree of covalence of the Al_4-O bonds with respect to Al_6-O ones.[24] This leads us to suggest that the substitution Si_{Al6} may be at the origin of the defect bands detected experimentally.[9,10] This is supported by the recent report of Lanza *et al.*[25] who have shown that a 1000 °C annealing treatment leads to the diffusion of Si from a native oxide SiO_2 layer into Al_2O_3. This is also in agreement with the thermal treatment (1000 °C).[26] required for the synthesis of aluminosilicates (clay) in which Si with its fourfold coordination has a nondisturbing stability in Al_2O_3. It implies that a proper control of the silicon diffusivity/thermal treatment is a key factor in the resolution of the reliability issues reported by Kerber *et al.*[8] However, the possibility of having a combination of several defects (for instance Si and C(C_{O4})) at the origin of the observed signature cannot be completely ruled out.

To conclude, we have computed the electronic signatures of a set of possible intrinsic and extrinsic defects present in γ-Al_2O_3 and compared them to the electrical characterization measurements reported by Degraeve[9] and Zahid *et al.*[10] We have found that among the sources of potential defects, the diffusion of Si in Al_2O_3 and the substitution of aluminum centers lead to defect levels whose positions in the band gap are close to the one detected experimentally.

This work is part of the IMEC Industrial Affiliation Program on nonvolatile memories.

[1] G. D. Wilk, R. M. Wallace, and J. M. Anthony, J. Appl. Phys. **89**, 5243 (2001).
[2] J. A. Kittl, K. Opsomer, M. Popovici, N. Menou, B. Kaczer, X. P. Wang, C. Adelmann, M. A. Pawlak, K. Tomida, A. Rothschild, B. Govoreanu, R. Degraeve, M. Schaekers, M. B. Zahid, A. Delabie, J. Meersschaut, W. Polspoel, S. Clima, G. Pourtois, W. Knaepen, C. Detavernier, V. V. Afanas'ev, T. Blomberg, D. Pierreux, J. Swerts, P. Fischer, J. W. Maes, D. Manger, W. Vandervorst, T. Conard, A. Franquet, P. Favia, H. Bender, B. Brijs, S. Van Elshocht, M. Jurczak, J. Van Houdt, and D. J. Wouters, Microelectron. Eng. **86**, 1789 (2009).
[3] G. Molas, M. Bocquet, E. Vianello, L. Perniola, H. Grampeix, J. P. Colonna, L. Masarotto, F. Martin, P. Brianceau, M. Gely, C. Bongiorno, S. Lombardo, G. Pananakakis, G. Ghibaudo, and B. De Salvo, Microelectron. Eng. **86**, 1796 (2009).
[4] B. O'Connor, D. Li, B. K. Gan, B. Latella, and J. Carter, Adv. X-Ray Anal. **41**, 659 (1999).
[5] T. C. Chou and T. G. Nieh, J. Am. Ceram. Soc. **74**, 2270 (1991).
[6] C. K. Lee, E. Cho, H.-S. Lee, K. Seol, and S. Han, Phys. Rev. B **76**, 245110 (2007).
[7] C. H. Lee, K. I. Choi, M. K. Cho, Y. H. Song, K. C. Park, and K. Kim, Tech. Dig. - Int. Electron Devices Meet. **2003**, 613.
[8] A. Kerber, E. Cartier, R. Degraeve, L. Pantisano, P. Roussel, and G. Groeseneken, Dig. Tech. Pap. - Symp. VLSI Technol. **2002**, 76.
[9] R. Degraeve, M. J. Cho, B. Govoreanu, B. Kaczer, M. Zahid, J. Van Houdt, and M. Jurczak, Tech. Dig. - Int. Electron Devices Meet. **2008**, 775.
[10] M. B. Zahid, A. Arreghini, R. Degraeve, B. Govoreanu, A. Suhane, and J. Van Houdt, IEEE Electron Device Lett. **31**, 1158 (2010).
[11] R. W. Godby, M. Schlüter, and L. J. Sham, Phys. Rev. Lett. **56**, 2415 (1986); P. Rinke, A. Qteish, J. Neugebauer, C. Freysoldt, and M. Scheffler, New J. Phys. **7**, 126 (2005); P. Rinke, A. Qteish, J. Neugebauer, and M. Scheffler, Phys. Status Solidi B **245**, 929 (2008).
[12] S. Kümmel and L. Kronig, Rev. Mod. Phys. **80**, 3 (2008).
[13] L. Hedin, Phys. Rev. **139**, A796 (1965).
[14] X. Gonze, B. Amadond, P.-M. Anglade, J.-M. Beuken, F. Bottin, P. Boulanger, F. Bruneval, D. Caliste, R. Caracas, M. Coté, T. Deutsch, L. Genovese, Ph. Ghosez, M. Giantomassi, S. Goedecker, D. R. Hamann, P. Hermet, F. Jollet, G. Jomard, S. Leroux, M. Mancini, S. Mazevet, M. J. T. Oliveira, G. Onida, Y. Pouillon, T. Rangel, G.-M. Rignanese, D. Sangalli, R. Shaltaf, M. Torrent, M. J. Verstraete, G. Zerah, and J. W. Zwanziger, Comput. Phys. Commun. **180**, 2582 (2009).
[15] P. E. Blöchl, Phys. Rev. B **50**, 17953 (1994).
[16] J. P. Perdew, K. Burke, and M. Ernzerhof, Phys. Rev. Lett. **77**, 3865 (1996); **78**, 1396(E) (1997).
[17] R. W. Godby and R. J. Needs, Phys. Rev. Lett. **62**, 1169 (1989).
[18] G. Paglia, C. E. Buckley, A. L. Rohl, B. A. Hunter, R. D. Hart, J. V. Hanna, and L. T. Byrne, Phys. Rev. B **68**, 144110 (2003).
[19] E. Menéndez-Proupin and G. Gutiérrez, Phys. Rev. B **72**, 035116 (2005).
[20] B. Ealet, M. H. Elyakhloufi, E. Gillet, and M. Ricci, Thin Solid Films **250**, 92 (1994).
[21] D. Liu and J. Robertson, Microelectron. Eng. **86**, 1668 (2009)
[22] J. Robertson, Rep. Prog. Phys. **69**, 327 (2006).
[23] J. R. Weber, A. Janotti, and C. G. Van de Walle, Microelectron. Eng. **86**, 1756 (2009).
[24] H. P. Pinto, R. M. Nieminen, and S. D. Elliott, Phys. Rev. B **70**, 125402 (2004).
[25] M. Lanza, M. Porti, M. Nafria, X. Aymerich, G. Benstetter, E. Lodermeier, H. Ranzinger, G. Jaschke, S. Teichert, L. Wilde, and P. Michalowski, Microelectron. Eng. **86**, 1921 (2009).
[26] F. S. Ohuchi, S. Ghose, M. H. Engelhard, and D. R. Baer, Am. Mineral. **91**, 740 (2006).